Synthesis and Characterization of Cobalt Ferrite Nanoparticles

A Thesis

submitted in partial fulfillment of the requirements for the award of the degree of

Master of Science in Physics

in

School of Physics and Material Science

Submitted by
Alisha Rohal
(Reg. No: 301604003)

Under the guidance of
Dr. B.N. Chudasama
Associate Professor

Thapar Institute of Engineering and Technology
Patiala-147004, Punjab, India

June 2018

CERTIFICATE

I hereby certify that the work, which is being presented in the thesis, titled **Synthesis and Characterization of Cobalt Ferrite Nanoparticles**, in partial fulfillment of the requirements for the award of the degree of **Master of Science in Physics** and submitted to the institution is an authentic record of my own work carried out during the period **Jan 2018** to **June 2018** under the supervision of **Dr. B. N. Chudasama**. I have also cited the reference about the text(s) from where they have been sourced.

The matter presented in this thesis has not been submitted elsewhere for the award of any other degree or diploma from any institution.

Alisha Rohal

(301604003)

This is to certify that the above statement made by the candidate is correct to the best of my knowledge.

Dr. B.N. Chudasama

Associate Professor and Supervisor

School of Physics and Material Science

Thapar Institute of Engineering and Technology

ACKNOWLEDGEMENT

Firstly, I would like to express my deep gratitude to my supervisor **Dr. B. N. Chudasama** for his invaluable advice and encouragement at every step of my thesis work. Without his unfailing support and belief in me, this thesis would not have been possible. His contribution to this work goes well beyond his role as an academic supervisor and includes constant support on a personal level and I am truly grateful for this.

I also thank **Dr. Manoj K. Sharma**, Professor and Head, School of Physics and Material Science, for his support and for providing me infrastructural facilities to conduct this research.

Special thanks to **Ms. Navjot Kaur**, Research Scholar, without her this thesis would have not been possible. She was always willing to listen, discuss and advice me throughout the work.

I owe more than thanks to my family members which includes my parents and brother, for their support and encouragement throughout my life. Words cannot express how grateful I am for their love, prayers and sacrifices for educating and preparing me for my future. Finally, I thank almighty God for giving me power to follow the right direction in achievement of my goal.

Alisha Rohal

ABSTRACT

Coprecipitation method is widely used to synthesize ferrite nanoparticles. Effect of pH, reaction temperature, annealing temperature and zinc substitution on the structural and magnetic properties of the cobalt ferrite and zinc substituted cobalt ferrite nanoparticles is studied in this thesis by x-ray diffraction (XRD) and vibrating sample magnetometer (VSM). The crystallite size ranges from 26.50 to 128.92 nm with increasing pH and from 26.50 to 128.92 nm with increasing reaction temperature. A gradual increase in crystallite size is observed with increasing zinc content although it is much less than the as-synthesized cobalt ferrite nanoparticles. Magnetic properties of the samples are also affected by reaction conditions. Saturation magnetization increases by increasing the reaction temperature as well as the sintering temperature. Coercivity ranges from 16.02 to 1247.32 Oe and remanence from 0.14 to 11.63 emu/g of the series obtained with increasing pH. No particular trend is detected as coercivity ranges from 88.49 to 431.14 emu/g and remanence from 0.73 to 8.99 Oe with the increasing reaction temperature. While both remanence and coercivity shows maximum values when the samples are annealed at 800 ^{o}C. Also an increasing trend of saturation magnetization with increasing annealing temperature is observed. The zinc substituted cobalt ferrite nanoparticles are superparamagnetic in nature and have maximum saturation magnetization of 38.98 emu/g with zinc content of 0.4.

TABLE OF CONTENTS

LIST OF FIGURES

LIST OF TABLES

ABBREVATIONS AND NOTATIONS

Co	Cobalt
Zn	Zinc
M	Molar mass
M^{2+}	Divalent metal ion
M^{3+}	Trivalent metal ion
Fe^{3+}	Ferric cation ion
MNPs	Magnetic nanoparticles
FCC	Face centred cubic
M	Molar mass
XRD	X-Ray Diffraction
VSM	Vibrating Sample Magnetometer
M_s	Saturation magnetization
M_r	Remanent magnetization
H_c	Coercivity
H_2O	Water
OH^-	Hydroxide
NaOH	Sodium hydroxide
$Fe_2^{3+}O_4^{2-}$	Iron oxide
$M^{2+}\ Fe_2^{3+}O_4^{2-}$	Mixed metal oxide
$FeCl_3$	Anhydrous ferric chloride
$C_4H_6CoO_4.4H_2O$ NaOH	Cobaltous acetate
$ZnFe_2O_4$	Zinc ferrite
$ZnSO_4.7H_2O$	Zinc sulphate heptahydrate
D	Crystallite size
RT	Room Temperature

ABBREVATIONS AND NOTATIONS

Symbol	Unit	Quantity
nm	nanometer	Length
gm	gram	Mass
mL	milliliter	Volume
M	molar	Mass
^{o}C	degree Celsius	Temperature
hrs	hours	Time
emu/g	electromagnetic unit per gram	Mass magnetization
Oe	oersted	Magnetic field
a.u.	arbitrary unit	Intensity

CHAPTER 1 INTRODUCTION

1.1 Nanoscience and Nanotechnology

The limelight of modern technology is Nanoscience and Nanotechnology. Nanoscience is an integrated field of physics, chemistry and biology. It deals with materials at the nanometre scale that ranges between 1 to 100 nm. An example of this scale range is illustrated through Figure 1.1. Nanoscience is not just limited to miniaturisation of materials, it is beyond that. A whole new physical phenomenon occurs at this small dimension and the properties of the material drastically changes with the dimension.

Nanotechnology is the implementation of these fabricated, characterized and explored nanomaterials for the development of technology. Size dependent property of nanomaterials has enabled a nanotechnology that engineers the properties of materials. Its applications cover a wide range of areas like health care, cosmetics, optics, biomedicines, electronics, etc.

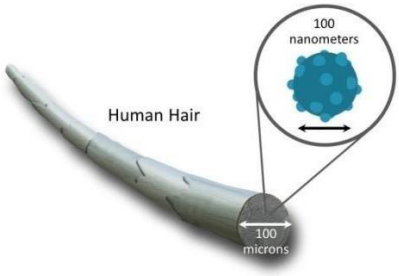

Figure 1.1 A human hair representing the idea of nanometre scale.

Nanoparticles are the materials falling in the nanometre scale range. Their history can be traced down from the early cultures of Egypt and Rome, where people used colloidal gold for making their ornaments [1]. Lately in 1857, Michael Faraday reduced gold in solution with white phosphorous to prepare red gold sols. He scientifically evaluated them and called them as divided metals [2]. By 20 th century, there was a great advancement in methods to synthesize colloidal gold [3]. After this many great works were followed like Bedrig used electrochemical method [4] and Zsigmondy discovered seeding method [5]. Lately, there has been an exponential development in the field of nanoscience because of the accessibility of new strategies and devices for characterization and additionally their applications in various fields.

1.2 Properties of Nanoparticles

When a bulk crystal reduces to nanometre size, the continuous bands in its electronic structure change to discrete or quantized bands. As a result, the properties of the molecules become size controlled because even the continuous optical transitions become quantized [6]. Properties of particles like electronic absorption and melting point is determined by the size of quantum dot. In magnetic materials, a whole new phenomenon of superparamagnetism has evolved due to this size effects. Whereas in metals, an unexpected catalytic activity is observed in particles having diameter size of 1 - 2 nm [7].

1.2.1 Electronic Properties of Nanoparticles

On the basis of their capacity to conduct electrical charge, bulk solid materials are classified as conductors, semiconductors and insulators. In insulators, overlapping of conduction and valence bands enables them to conduct electrons. In semiconductors, valence bands are fully filled while conduction bands are empty with small energy gap. Through thermal or optical excitation, the movement of electrons to conduction band from valence band is conceivable. In case of insulators, large band gap incapacitates this movement. While at nanometre scale, the metal sample becomes insulating because the continuous band breaks down. For semiconductor nanoparticles, increase in band gap is observed because energy levels become discrete at the band edge with some inter level spacing. Such changes are known as quantum size effects [8]. Many such size dependent changes have been observed in absorption spectra of semiconducting nanomaterials.

1.2.2 Magnetic Properties of Nanoparticles

Magnetic properties that are size dependent are usually found when the material size ranges between few microns to few nanometres. A multi domain structure exists in bigger particles, where uniform magnetization regions are isolated by domain walls as shown in Figure 1.2 (a). Magnetization of these regions can be reversed by shifting these domain walls. With the decrease in particle size, a single domain state is formed in which alignment of all spins are in the same direction as shown in Figure 1.2 (b).

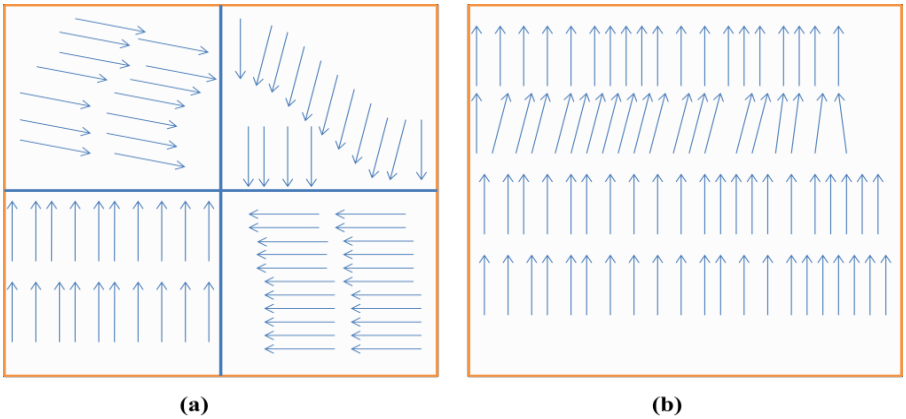

Figure 1.2 The different domain states existing in a particle (a) multi-domain particle separated by domain walls and (b) single domain particle.

The coercivity of a particle initially increases with decrease in particle size till a critical diameter is reached [9]. However, there is decrease in coercivity below this critical diameter due to the thermal effects. This phenomenon is called superparamagnetism [10]. The variation of coercivity with diameter of the particle is schematically shown in Figure 1.3. Superparamagnetic particles show magnetic properties identical to their bulk counterpart at low temperature and have little or no coercivity at high temperature.

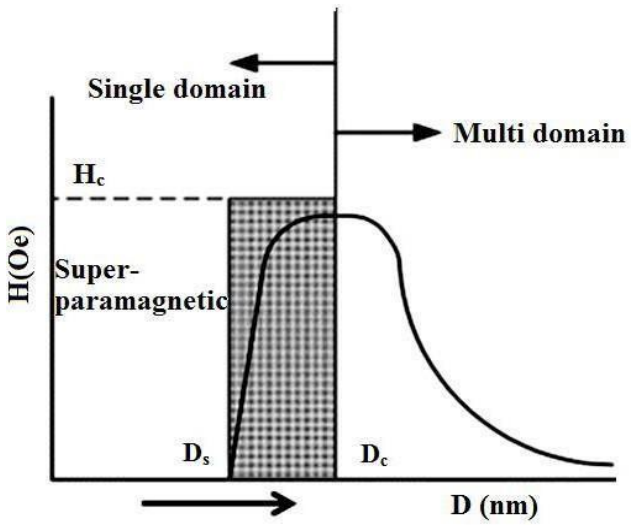

Figure 1.3 Illustration of coercivity variation of a particle with diameter.

Superparamagnetic state is achieved by nanoparticles when their magnetization is a single magnetic moment for each particle rather than individual atomic moment [10]. This behaviour where magnetic properties are dependent on a preferred direction is known as magnetic anisotropy. Superparamagnetic materials exhibit high saturation magnetization while zero coercivity and remanence. This enables control over their

movement in external magnetic field, leading to various applications in biomedicine [11].

1.3 Ferrites

The ceramic compounds consisting of a chemical combination of iron oxide with one or more metals are known as ferrites [12]. They are the metal oxide containing magnetic ions grouped together to produce spontaneous magnetization [13]. Their molecular formula is $M^{2+}Fe_2^{3+}O_4^{2-}$ in which M stands for divalent metals like Co, Zn, etc. Ferrites exhibit properties like high electrical resistivity, magnetic permeability and saturation magnetization but low dielectric losses. Such differing properties makes ferrites one of a kind and empowers it to be utilized as a part of an extensive variety of uses like transformers, magnetic resource imaging, permanent magnets, magnetic refrigeration, etc. [14]

1.4 Classification of Ferrites

Ferrites are classified into two sub-categories:

1.4.1 Soft Ferrites

Soft ferrites are the ones that are easy to magnetize and demagnetize, thereby making them non acceptable for permanent magnets. Soft ferrites have narrow hysteresis loops as compared to hard ferrites. They have low coercivity and remanent magnetization while high susceptibility and saturation magnetization. Also the eddy current losses are very low due to high resistivity. They are mainly used to make transformer cores [15].

1.4.2 Hard Ferrites

Hard ferrites are the ones that are difficult to magnetize and demagnetize, making them ideal for permanent magnets. Cobalt ferrite and barium ferrite are a few examples. Their hysteresis curve is broader than the soft ferrites which can be seen in Figure 1.4. They have low saturation magnetization while high coercivity and remanent magnetization, unlike soft ferrites. They are mainly used in automobiles, electric motors, etc. [15]

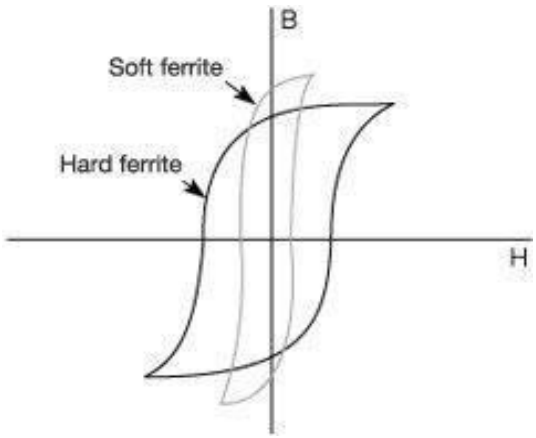

Figure 1.4 Hysteresis loops of soft ferrites and hard ferrites.

1.5 Structure of Ferrites

1.5.1 Spinel Ferrites

Spinel ferrites, known as cubic ferrites are represented by the chemical formula MFe_2O_4. They have FCC unit cell with eight formulas in per unit cell which modifies its chemical formula as $M_8Fe_{16}O_{32}$. Because of their low eddy current losses and high electrical resistivity, they are most commonly used at microwave frequencies [16]. Based on their cationic appropriation on tetrahedral and octahedral sites, spinel ferrites are classified into subgroups:

a) Normal Spinel

In normal spinel structure, one kind of cations sit at the octahedral sites [17]. They have formula $M^{3+}M^{2+}M^{3+}O_4$, in which M^{2+} represents a divalent metal occupying the tetrahedral sites and M^{3+} represents a trivalent metal occupying the octahedral sites as shown in Figure 1.5.

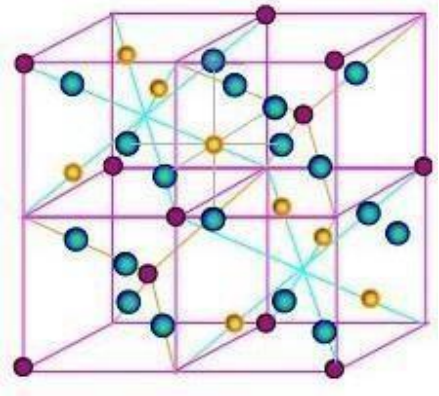

Figure 1.5 A spinel ferrite structure. Here purple spheres represent Cobalt, yellow spheres represent Iron and blue spheres represent Oxygen.

b) Intermediate Spinel

These are random spinel structures having an arbitrary distribution of divalent and trivalent cations on their tetrahedral and octahedral sites. Number of cations on both the sites is unequal [18].

c) Inverse Spinel

In inverse spinel structure, fifty percent of the trivalent ions occupy the tetrahedral sites while the remaining fifty percent of trivalent and all divalent ions occupy the octahedral sites [19]. Its structural formula is given as $M^{3+}M^{2+}M^{3+}O_4$, where M^{2+} represents a divalent metal and M^{3+} represents a trivalent metal occupying both the tetrahedral and octahedral sites as shown in Figure 1.6.

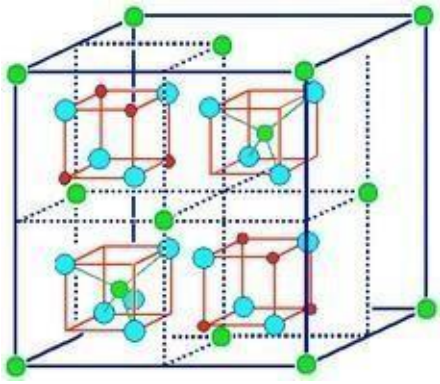

Figure 1.6 An inverse spinel ferrite structure. Here red atoms represent octahedral sites, green atoms represent tetrahedral sites and blue atoms represent Oxygen.

1.6 Cobalt Ferrites

Among the immense technological applications at nanoscience, cobalt ferrite ($CoFe_2O_4$) with inverse spinel structure proves to be a promising magnetic nanoparticle. Cobalt ferrite exhibits high coercivity and electrical properties while has good chemical stability and mechanical properties. Its structure is shown in Figure **1.7** which has Co cation occupying half of its octahedral sites (B) while rest half of it and all the Fe^{3+} cations occupies the tetrahedral sites (A) [20]. Its saturation magnetization decreases with size and is always less than that of bulk. Coercivity reaches maximum value when its crystallite size and single domain size becomes approximately equal. It is used in targeted drug delivery, magnetic resonance imaging, audio and video tapes, etc. [21].

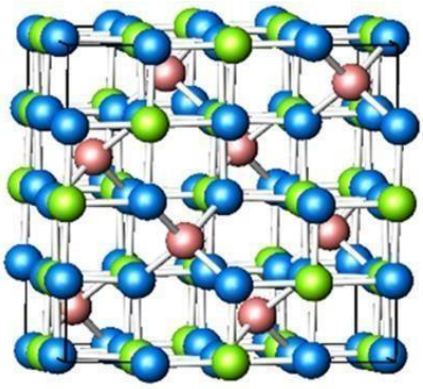

Figure 1.7 Crystal structure of $CoFe_2O_4$ in which green atoms represent Cobalt, pink atoms represent Iron while blue atoms represent Oxygen.

1.7 Synthesis of Magnetic Nanoparticles

Nanoparticles can be synthesized by various techniques, each having their own advantages. The requirement of materials and morphology of nanoparticles depend on their applications. Two basic approaches are top-down and bottom-up which are illustrated in Figure1.8.

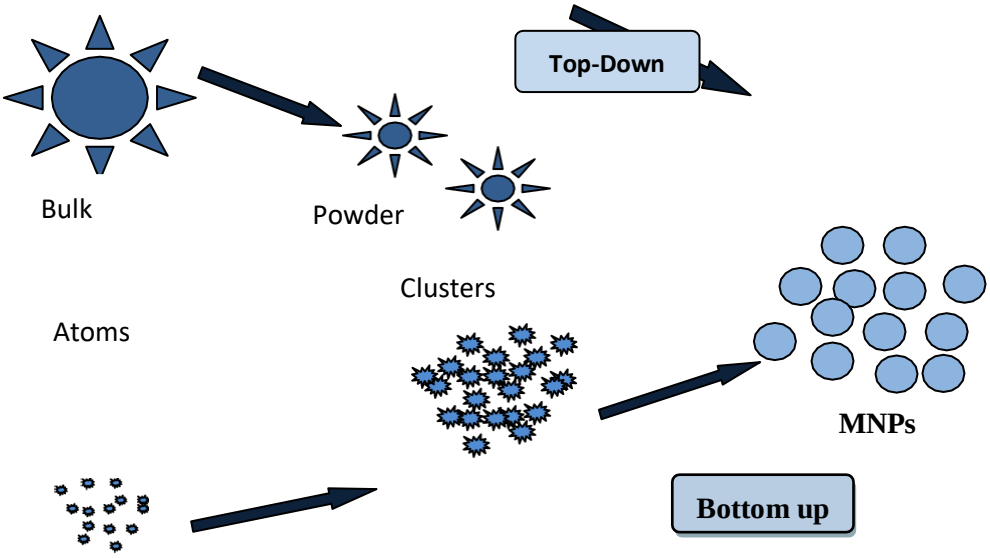

Figure 1.8 A schematic representation of top-down and bottom-up approaches of synthesis of nanoparticles.

The basic approach is further classified into physical, chemical and biological methods that have their respective techniques, as listed in Figure1.9.

Magnetic nanoparticles can be synthesized by several methods with different composition and phases. Few methods are coprecipitation, thermal decomposition, hydrothermal, micro-emulsion, etc.

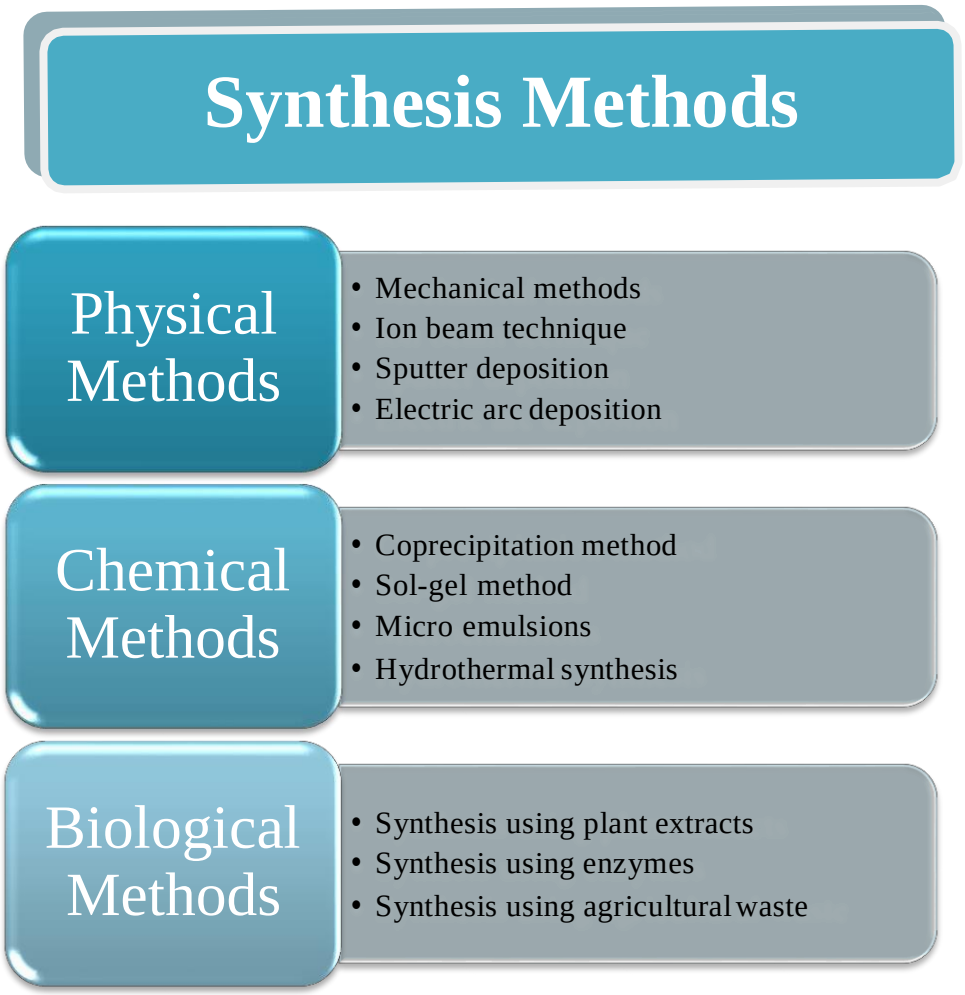

Figure 1.9 Physical, chemical and biological methods of nanoparticle synthesis.

1.8 Coprecipitation Method

Magnetic nanoparticles like cobalt ferrites can be synthesized by coprecipitation method, which is a very convenient technique for nanoparticle synthesis. In this method, aqueous salts of $Fe^{3+}$and its corresponding divalent cation are used to prepare ferrite nanoparticles by adding base at a suitable temperature to the acidic solution. The resultant particles can vary in composition, shape and size, therefore it depends on factors like temperature, pH, type of salts and surfactants.

Ferrite nanoparticles formed by this method is given by the following equation:

$2Fe^{3+} + M^{2+} + 8OH^{-} \rightarrow MFe_2O_4 + 4H_2O$

Different morphologies of nanoparticles like spherical, cubical, rods, etc have been formed using this method.

1.9 Zinc Substitution in Cobalt Ferrite Nanoparticles

Cobalt ferrite nanoparticles are a fascinating area of research due to their peculiar properties like large anisotropy, coercivity and high saturation magnetization. But when we substitute Co^{2+} in this ferrite with Zn^{2+}, a slight modification in its magnetic properties can be observed. In this thesis, a detailed study on the effect of zinc substitution in cobalt ferrites is done. Zinc iron oxide ($ZnFe_2O_4$) has its structure as normal spinel where Zn^{2+} ions occupy tetrahedral sites while Fe^{3+} ions occupy octahedral sites [22]. Cobalt ferrite ($CoFe_2O_4$) on the other hand has its structure as inverse spinel in which Co^{2+} ions occupies octahedral sites and Fe^{3+} ions are equally distributed in tetrahedral and octahedral sites. Hence when we substitute Zn in $CoFe_2O_4$, it leads to a distorted spinel structure.

CHAPTER 2 LITERATURE REVIEW

From the last several years, synthesis and characterization of magnetic nanoparticles have been a fascinating theme of research. $CoFe_2O_4$ magnetic nanoparticles can be synthesized by numerous procedures, for example, coprecipitation, thermal decomposition, reverse micelle, sol-gel, combustion method, hydrothermal method, etc.

Zhao et al. [2007] used hydrothermal method to prepare cobalt ferrite nanoparticles. Particles with 5 nm of average diameter were prepared at 390 °C. Low coercivity and high magnetic saturation was observed in particles synthesized by this method as compared to other methods. The maximum value of coercivity was 340.6 Oe and saturation magnetization was 68.9 emu/g [23].

Naseri et al. [2010] prepared the spinel $CoFe_2O_4$ nanoparticles by thermal treatment. Calcination temperature was from 623 K to 923 K. The observed particle sizes were 12.5 – 39 nm. With increase in temperature, saturation magnetization and remanence increases while coercivity decreases after becoming maximum [24].

Vazquez et al. [2011] prepared cobalt ferrite nanoparticles using non-aqueous solvo-thermal method. The average particles size was in the range 2 - 15 nm and indicated a superparamagnetic behavior from their magnetic studies. It was observed that with decrease in temperature, the magnetic properties increases. Also small size of nanoparticles lead to surface spin effects and enhanced finite size[25].

Gandha et al. [2015] synthesized $CoFe_2O_4$ NPs using hydrothermal technique. It was found that by varying synthesis parameters, the particle size can be controlled from 20 - 100 nm. At 300K, M_s of 73 emu/g and H_c of 5 kOe were obtained which were maximum values reported through one - step hydrothermal method [26]. From the above survey, we can conclude that hydrothermal method is a very simple technique to implement. The nanoparticles size as well as properties can also be controlled by it. But the need of expensive autoclaves is a major drawback.

Sol-gel, auto combustion method has edge over this method due to the following reasons: (a) the rapid heating to treatment temperature helps in saving time as well as energy (b) the reaction kinetics are enhanced by few order of magnitude (c) leads to novel phase formation (d) leads to selective crystallization. This method is also known as solution combustion method because of the combination of chemical

sol-gel and the combustion process. It has a major contribution in preparing spinel type ferrite nanoparticles.

Toksha et al. [2008] used sol-gel auto combustion method for the synthesis of $CoFe_2O_4$ nanoparticles. The crystal structure of the particles was inverse spinel with lattice constant 158 Å and average particle size was 15 nm. At room temperature, saturation magnetization was 67emu/g, coercivity was 1215 Oe and remanence was 30.2 emu/g. While at 77K, saturation magnetization was 43 emu/g, coercivity was 10.2 kOe and remanence was 35 emu/g. The particle size was found to increase with increasing annealing temperature and time [27].

Singhal et al. [2010] used the sol-gel method to synthesize Zn substituted $CoFe_2O_4$ NPs. The particle size was observed to be approximately 10 nm which when annealed upto 1000 °C was found to increase upto 92 nm. Also a linearly increasing trend was found in the lattice parameter with the increasing concentration of Zn. M_s firstly increases but then decreases for higher Zn substitution in the nanoparticles [28].

Sajjia et al. [2014] followed sol-gel technique to prepare cobalt ferrite nanoparticles assuming a correlation between structural properties of material and heat treatment operation parameters. The particle size distribution was estimated in the range 7-28 nm with heat treatment parameters as 250 °C and 10 hrs. A ferromagnetic behaviour was observed at room temperature with saturation magnetization62 emu/g[29].

Raut et al. [2014] prepared Co-Zn ferrite NPs using sol-gel auto combustion method. The cubic spinel structure observed was single phase and crystallite size varied with zinc concentration in the range 45 - 49 nm. The data obtained gave M_s, M_r and H_c as 65.628 emu/g, 71.929 emu/g and 1116.9 Oe respectively, which indicated its decreasing trend with increasing Zn concentration [30].

Prabhakaran et al. [2016] followed combustion route to synthesize cobalt ferrite nanoparticles. The prepared samples were annealed for 2 hrs at 500 and 800 °C to observe temperature effect on various magnetic properties. It was found that the samples exhibit cubic spinel structure. Also, average particle size was 37.8 and 43.7 nm, M_s was 61 and 69 emu/g and M_r was 29.75 and 31.53 emu/g for 500 and 800 °C, respectively [31].

Recently, Ashour et al. [2018] synthesized metal substituted $CoFe_2O_4$ NPs using a sol-gel technique. The crystallite size with the integration of metals i.e. Zn and

Cu ranges from 13.04 nm to 33.71 nm respectively. A cubic spinel structure was observed even after the substitution of metals. With the increasing annealing temperature, the particle size increases [32].

Senthil et al. [2018] used auto combustion sol-gel method to synthesize cobalt ferrite nanoparticles. The calcination temperatures i.e. 600, 700 and 800 °C gave crystallite sizes of the samples as 50, 65 and 80 nm respectively. From the observations, the increase in calcination temperature was found to increase the value of M_s from 23 to 63 emu/g and that of coercivity from 90 to 203 Oe [33].

Morais et al. [2001] synthesized $CoFe_2O_4$ NPs using coprecipitation technique. It was detected that the particle size could be controlled by different stirring speeds. The data obtained showed that the particle diameter reduced from 15.1 to 11.4 nm by increasing the speed of stirring from 2700 to 8100 rpm. Also the nanoparticles exhibited superparamagnetic behaviour [34].

Chinnasamy et al. [2002] prepared $CoFe_2O_4$ nanoparticles by a growth dominant coprecipitation process. The consequences of reaction temperature, NaOH concentration and feeding rate of metal ions were studied separately during the process. At 98 °C, the maximum saturation magnetization of 2.29 emu/g was observed. Also the average particle size was between 14 - 20 nm and maximum coercivity was 4.3 kOe at room temperature [35].

Kim et al. [2003] used temperature controlled coprecipitation method for the synthesis of $CoFe_2O_4$ NPs, where the temperature range was set between 20- 80 °C. A broad and unresolved peak of samples at 20 °C and 40 °C was detected whereas a clear pattern on the other hand at 60 °C and 80 °C was also found. This pattern corresponded to a lattice of cubic spinel type. The data obtained gave average particle size of 2 to 15 nm and M_s from 2-58.3 emu/g, which showed that both these parameters increase with increasing synthesis temperature [36].

Yuqiu et al. [2006] synthesized $CoFe_2O_4$ NPs by coprecipitation technique at different temperatures. It was detected that with increase in reaction temperature, particle size increases from 2.4 – 47.4 nm within the temperature range of 40 - 100 °C. Also, there was an increase in saturation magnetization with increasing reaction temperature showing 29.5 emu/g at RT. Coercivity and remanence was found to be 3267 Oe and 0.58 emu/g, respectively which indicated their dependence on particle

size [37].

Gul et al. [2007] prepared zinc substituted cobalt ferrite NPs using coprecipitation method. The average particle size was within 12 - 16 nm at 70 °C and exhibited a cubic spinel structure. With increase in zinc concentration, the Curie temperature decreases [38].

Zi et al. [2009] used chemical coprecipitation method to prepare cobalt ferrite nanoparticles. It was found that the average crystallite was 8.56 nm. At room temperature, M_s was 61.77 emu/g and M_r was 15.39 emu/g. Also, low coercivity of 0.519 kOe was observed. It is due to the transformation from ferrimagnetic to superparamagnetic state [39].

Zhang et al. [2010] synthesized $CoFe_2O_4$ NPs by coprecipitation method in which the particles were heated at 90 °C for 2 hrs. Many samples were synthesized at different NaOH concentration. It was observed that the crystallite size increases and saturation magnetization decreases with the increase in sodium hydroxide concentration [40].

Mozaffari et al. [2010] adopted coprecipitation technique to prepare Zn substituted $CoFe_2O_4$ NPs. It was detected that with increasing solution temperature from RT to 363 K, the particle size also increases from 6 to 8 nm, respectively. The particles exhibited superparamagnetism at RT and attained no saturation even at maximum field [41].

Okr et al. [2011] prepared $CoFe_2O_4$ nanoparticles by coprecipitation method. Samples were synthesized within the temperature range of 20 – 80 °C whereas the one at 60 °C was kept for annealing at 500 – 900 °C for 2 hrs. It was found that within this range of temperature, the average particle size were 9.4 – 42.3 nm. It was observed that M_s, H_c and M_r also increase with increasing annealing temperature [42].

Huixia et al. [2014] used the reverse coprecipitation method to synthesize cobalt ferrite nanoparticles. Different pH and aging temperatures were used to prepare nanoparticles. From the data obtained it was found that with aging temperature, the particles size also increases whereas no particular trend was observed in saturation magnetization[43].

Tatarchuk et al. [2017] used chemical coprecipitation method to investigate the effect of Zn substitution in $CoFe_2O_4$ NPs. A cubic spinel structure with crystallite

size ranging from 46 to 77 nm was observed. It was found that with increasing Zn concentration, both H_c and M_r decreases while M_s first increases and then decreases. Amongst several synthesis techniques, coprecipitation method was found to be most easy, rapid and economical. Also, the reactant precipitates were mixed homogenously which helps in reducing the reaction temperature [44]. It has been observed that there is no precise pattern in the structural and magnetic properties of $CoFe_2O_4$ NPs. Distinctive synthesis techniques and preparation conditions gives different results. The correlation between synthesis parameters and structural and magnetic properties of NPs could not be established. Therefore in this thesis, it is aimed to synthesize cobalt ferrite and Zn substituted $CoFe_2O_4$ NPs and investigate their structural as well as magnetic properties.

2.1 Objectives

i. To prepare $CoFe_2O_4$ NPs using coprecipitation method by (a) varying pH (b) varying reaction temperature.

ii. To study the effect of varying annealing temperature on the prepared cobalt ferrite nanoparticle samples.

iii. To synthesize $CoFe_2O_4$ NPs with Zn substitution in it.

iv. To characterize as-synthesized $CoFe_2O_4$ nanoparticles and Zn substituted $CoFe_2O_4$ nanoparticles by XRD and VSM.

Chapter 3 SYNTHESIS AND CHARACTERIZATION

3.1 Synthesis of Cobalt Ferrite Nanoparticles

Materials used**:** $CoFe_2O_4$ NPs were synthesized by using cobaltous acetate ($C_4H_6CoO_4.4H_2O$), anhydrous ferric chloride ($FeCl_3$) and sodium hydroxide (NaOH) as the reagents. Milli-Q ultrapure distilled water was used in order to prepare all the aqueous solutions.

Method used: Coprecipitation method

Preparation procedure:

SETA ⟶ pH variation

STEP 1:- Take 0.01 M of cobaltous acetate (2.49 gm) and 0.02 M of anhydrous ferric chloride (3.24 gm) along with 0.08 M of sodium hydroxide (3.2 gm) in different beakers.

STEP 2:-Dissolve two salts in 100 mL of distilled water separately. Similarly, dissolve the base i.e. NaOH in 100 mL of distilled water. Prepare another beaker with 1.5 gm of NaOH dissolved in 30 mL of distilled water.

STEP 3:- Add salt solutions into 100 mL NaOH under stirring. Color changes from light red to brown.

STEP 4:- If required, excess NaOH solution is added drop wise into the mixture to adjust its pH between 10 and 13.

STEP 5:- This solution is allowed to stir mechanically for 20 mins, during which formation of metal hydroxides takes place.

STEP 6:- It is further subjected to heating at higher temperature (90 °C) for 3 hrs.

STEP 7:- After this, it is cooled to room temperature.

STEP8:- Magnetic decantation is done followed by washing several times using warm distilled water and once by acetone.

STEP 9:-It is then dried overnight in oven at 70 °C. Finally the prepared nanoparticles are grinded and preserved for further characterization.

The reaction taking place is as follows:

$$10\ mM\ C_4H_6CoO_4.4H_2O + 20\ mM\ FeCl_3 + 80mM NaOH \longrightarrow 10\ mM\ CoFe_2O_4$$

$$+ 60\ mM\ NaCl + 10\ mM\ Na_2(C_4H_6O_4) + 80\ mM\ H_2O$$

In this set, we prepared a series of $CoFe_2O_4$ NPs at 90 °C and pH 10, 11, 12 and 13. Hence, we obtained a series of $CoFe_2O_4$ NPs by varying pH.

SETB ⟶ Temperature variation

The above mentioned steps to prepare the samples are repeated in this set except *STEP 7*, where it is heated at 90 °C, instead this time temperature is fixed at 25 °C, 80 °C, 90 °C and 100 °C. The pH remains fixed at 11 for all samples.

In this set, we prepared cobalt ferrite nanoparticles at constant pH 11 and temperature 25 °C, 80 °C, 90 °C and 100 °C. Hence, we obtained a series of cobalt ferrite nanoparticles by varying temperature.

SETC ⟶ Annealing temperature

A sample of cobalt ferrite nanoparticles was prepared using all steps mentioned in SET A with preparation conditions as pH 11 and temperature 90 °C. The synthesized sample was divided into three equal parts, which were further annealed at 500 °C, 800 °C and 1100 °C, each for 12 hrs.
Hence we obtained a series of cobalt ferrite nanoparticles that was prepared at pH 11, temperature 90 ^{o}C and annealed at three temperatures i.e. 500 °C, 800 °C and 1100 °C. A flowchart of the above mentioned procedure is shown in Figure. 3.1.

SETD ⟶ Synthesis of zinc substituted cobalt ferrite

STEP 1:- Take 0.01 M of cobaltous acetate ($C_4H_6CoO_4.4H_2O$), 0.01 M of zinc sulphate heptahydrate ($ZnSO_4.7H_2O$), 0.02 M of anhydrous ferric chloride ($FeCl_3$) and 0.08 M of sodium hydroxide (NaOH) each in a different beaker.

STEP 2:- Dissolve each one of them in 100 mL of distilled water separately.

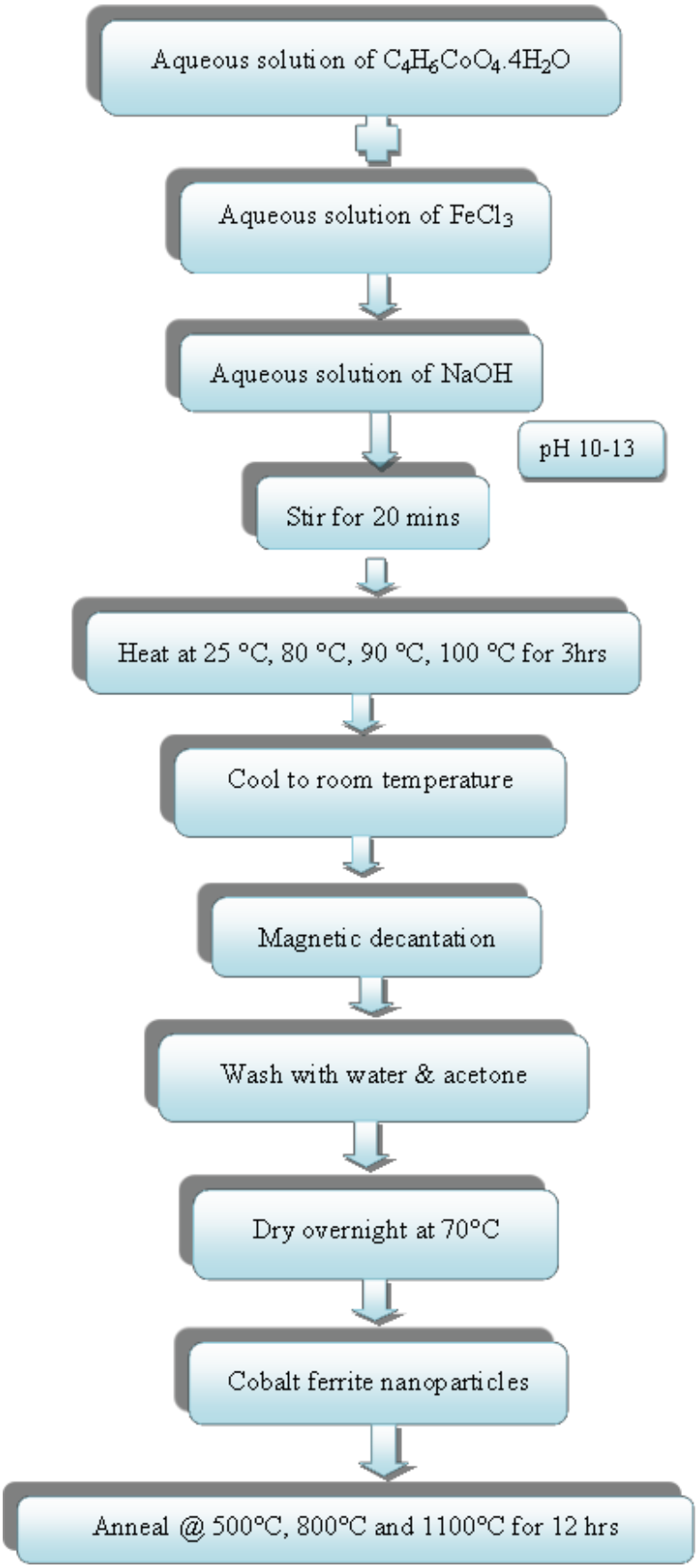

Figure 3.1 Synthesis route followed to prepare cobalt ferrite nanoparticles.

STEP 3:- Add 1.5 gm of NaOH in 30 mL of distilled water in another beaker.

STEP 4:- Mix the three acidic solutions together into a single beaker.

Repeat *STEPS 4 - 9* of SET A by fixing the pH at 11 and temperature 90 °C. Through this procedure, a sample of $Co_{0.8}Zn_{0.2}Fe_2O_4$ has been prepared. By further changing the amount of substitution of zinc, more samples were prepared by the above mentioned procedure. Finally we obtain a series of cobalt ferrite nanoparticles which are substituted with zinc as $Co_{1-x}Zn_xFe_2O_4$ (x= 0 - 1).

3.2 Characterization of Nanoparticles

Nanoparticles characterization involves several techniques to have a deeper knowledge about the synthesized particles and their properties. Two of them which are studied in this thesis are explained below:

3.2.1 X-ray Diffraction

X-rays are the electromagnetic radiations which undergo diffraction. XRD is a characterization method adopted to determine structure of crystalline material.

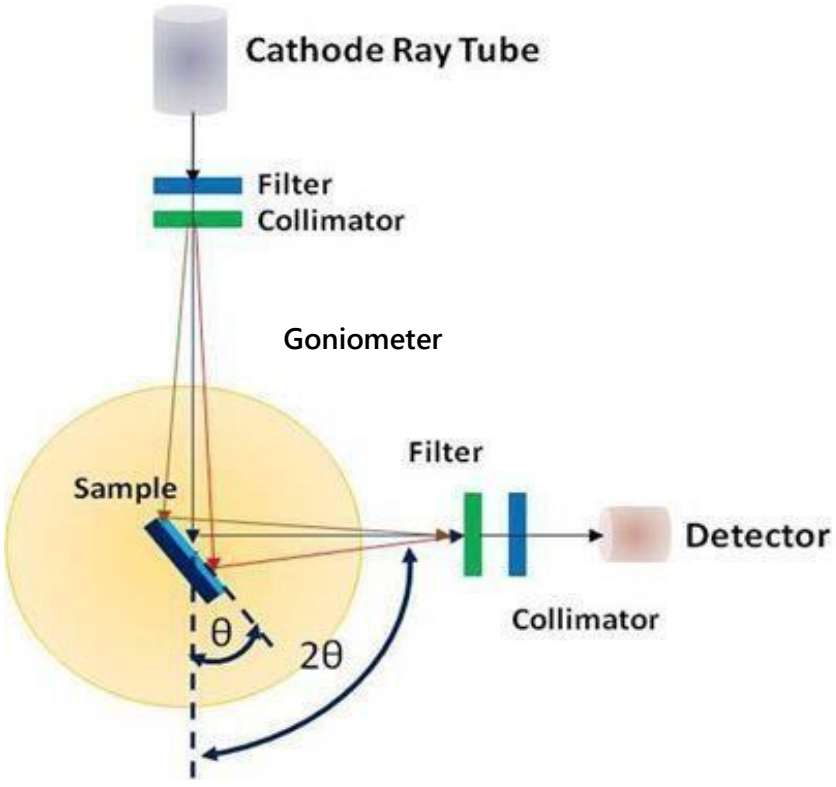

Figure 3.2 Schematic diagram of X-ray Diffractometer.

Other structural factors like atomic spacing, crystal orientation, average grain size, crystallinity can also be determined using this technique. The wavelength suitable for it ranges from few angstroms to 0.1 A^0. In this technique, crystalline material undergoes constructive interference with monochromatic x-rays. In XRD, mostly powder diffraction method is adopted in which the samples are used in powder form. Cathode ray tube produces filtered x-rays giving a monochromatic beam. This beam is then focussed on the sample [45]. Diffracted beams are deflected by an x-ray detector which is on goniometer at $2\theta^0$ angle, as shown in Figure 3.2.

Debye-scherrer method is used to determine the crystallite size which has the formula

$$d = k\lambda/ \beta\cos\theta$$

Where 'd' represents the crystallite size of nanoparticles, 'k' the Scherrer constant, 'λ' the wavelength of incident X-rays, FWHM of highest peak is given by 'β' and angle of diffraction is 'θ'. Bragg's law helps us to determine the inter-planar spacing which is schematically drawn in Figure 3.3 and is given by

$$2d\sin\theta = n\lambda$$

Where 'd' is inter-planar spacing, 'θ' is angle of diffraction, 'n' is diffraction order and 'λ' is wavelength of incident X-ray.

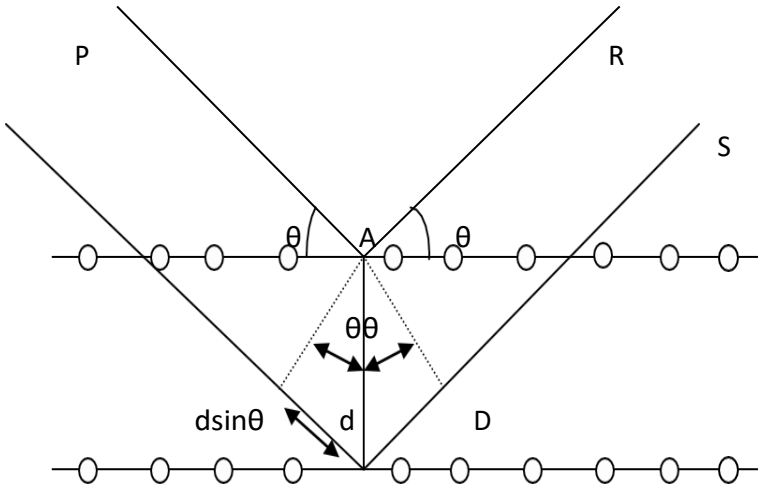

Figure 3.3 Schematic representation of x-ray diffraction from crystal lattice.

3.2.2 Vibrating Sample Magnetometer

VSM is the most appropriate magnetometer to measure magnetic properties of magnetic materials. It depends on Faraday's law. Whenever flux is changed through coil, electromagnetic force is induced in it. In VSM, a uniform magnetic field is created in which the material is placed. Magnetic moment is induced in the target material. This material starts vibrating when placed in sensing coils because of the uniform magnetic field. It induces magnetic flux voltage that equals the magnetic moment of sample. The applied magnetic field magnetizes the particles which enables the domains to be aligned. Its schematic representation is given in Figure 3.4. The stronger is the magnetic field, more will be the alignment of magnetic moment of the sample. This technique gives us a hysteresis loop which enables us to know about the magnetic properties of sample like M_s, M_r and H_c [46].

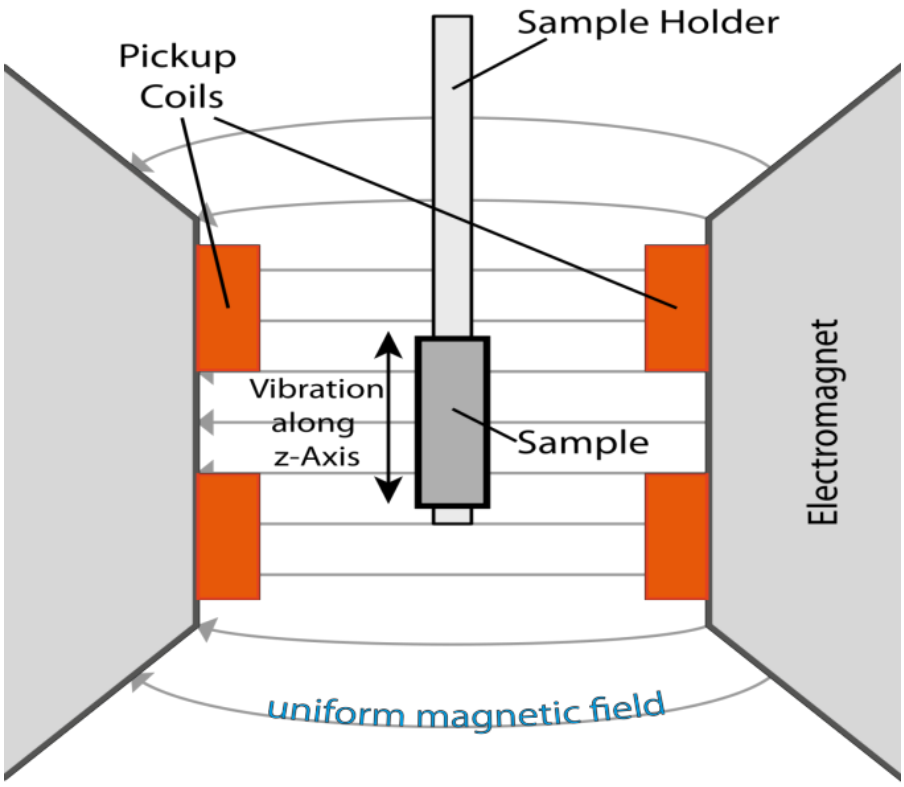

Figure 3.4 Schematic representation of a VSM.

Chapter 4 RESULTS AND DISCUSSIONS

4.1 X-Ray Diffraction

XRD patterns were measured using the x-ray diffraction technique with CuK_α radiation (λ=0.15406 nm) with 2θ within the range 30° – 40°. Percentage crystallinity and crystallite size are determined from the (311) reflection of inverse spinel structure.

4.1.1 Structural Properties of Cobalt Ferrite Nanoparticles

A series of $CoFe_2O_4$ NPs have been prepared which undergo XRD characterization at RT. The peak with highest intensity is observed.

(a) Variation in pH

The crystallite sizes of the NPs were evaluated by preparing a series of samples by varying its pH. Peak broadening occurs due to the small crystallite size which can be seen in the XRD pattern in Figure 4.1.

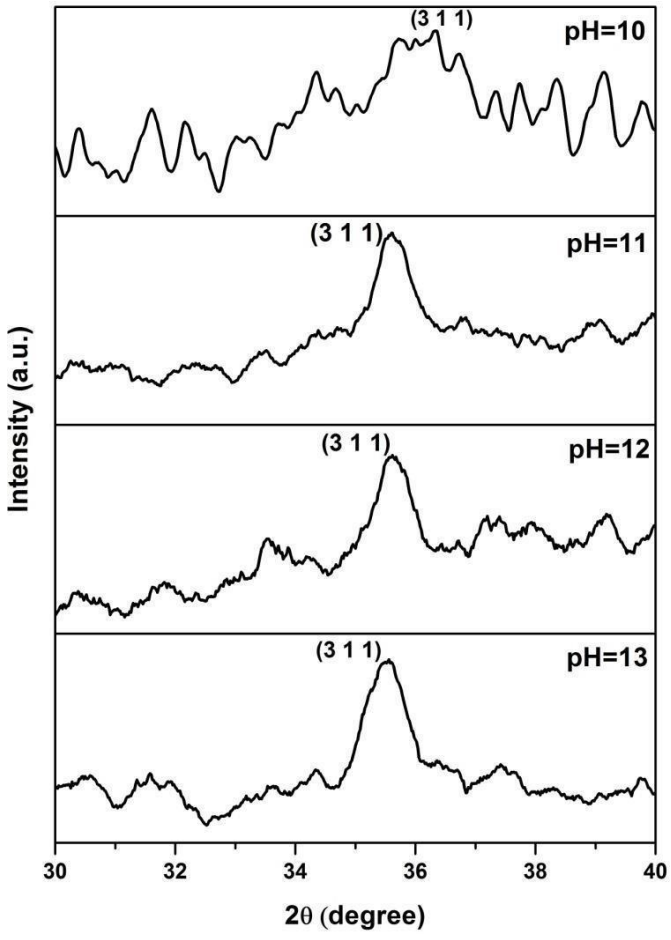

Figure 4.1 XRD pattern of the synthesized $CoFe_2O_4$ NPs with varying pH.

Only the highest peaks are taken in consideration for this analysis and its indexing is done well representing a cubic spinel structure. Scherrer method is used to calculate the crystallite size as explained in section 3.2.1. It is observed that the crystallite size of the samples show an increasing trend with increasing pH and then gradually decreases. It is maximum at 11 pH with a crystallite size of 128.92 nm. Its variation is shown in Table 4.1. The crystallinity percentage also increases with increasing pH.

Table 4.1 Crystallite sizes and % crystallinity of synthesized $CoFe_2O_4$ NPs as a function of pH.

pH	D (nm)	% crystallinity
10	26.50	79.68
11	128.92	84.03
12	114.09	86.07
13	101.80	81.32

(b) Variation in Reaction Temperature

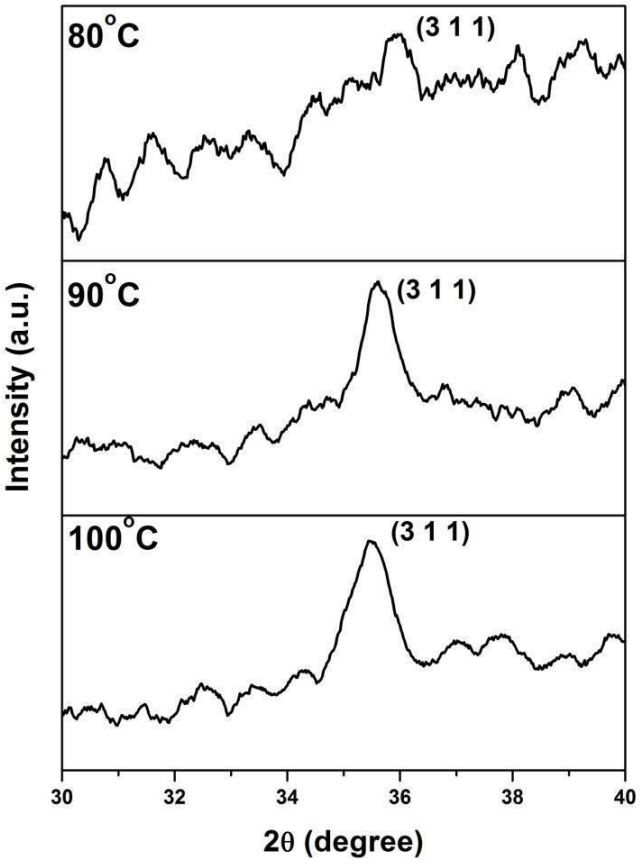

Figure 4.2 XRD pattern of the synthesized $CoFe_2O_4$ NPs with varying reaction temperature.

Another series of samples are prepared at different reaction temperature and the resulting XRD pattern are shown in Figure 4.2. Indexing of only the highest peak is done just like the previous series. The determined values of D are shown in Table 4.2. Crystallite size gradually decreases with increase in reaction temperature and is the highest for 90 ^{o}C. Percentage crystallinity on the other hand shows a decreasing trend.

Table 4.2 Crystallite size and % crystallinity of $CoFe_2O_4$ NPs as a function of reaction temperature.

T(^{o}C)	D (nm)	% crystallinity
80	29.4	92.66
90	128.92	84.03
100	106.93	80.72

4.1.2 Zinc Substitution in Cobalt Ferrite Nanoparticles

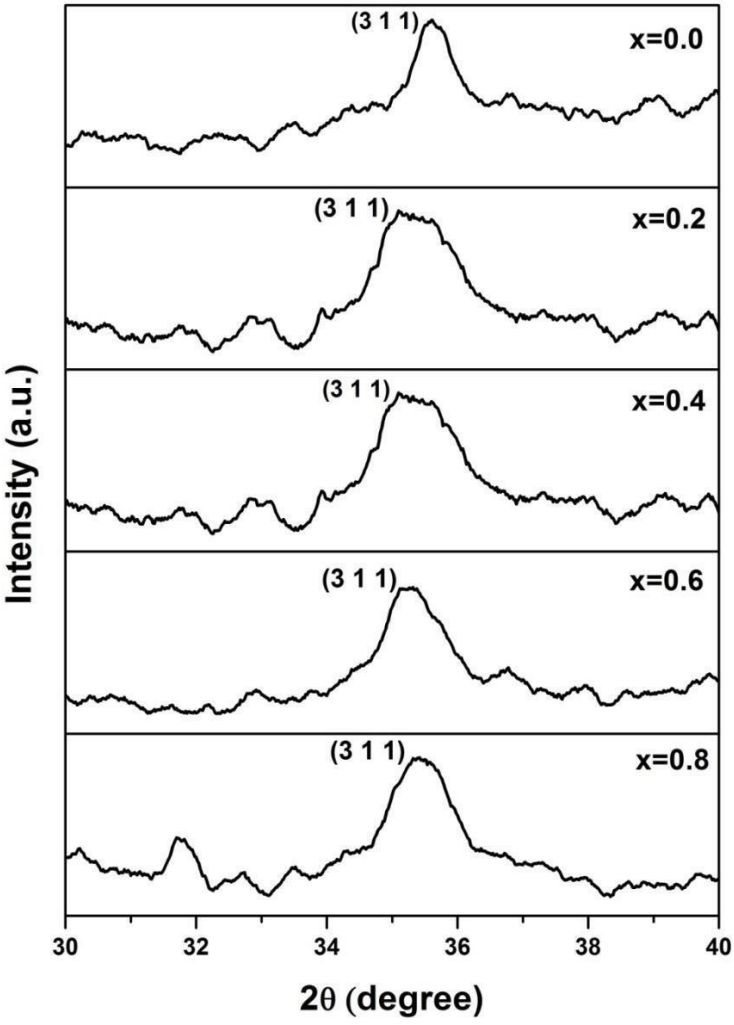

Figure 4.3 XRD pattern of the synthesized $CoFe_2O_4$ NPs with varying Zinc content.

The XRD patterns of $CoFe_2O_4$ NPs by substituting zinc ($Co_{1-x}Zn_xFe_2O_4$) with varying Zn content 'x' as $0.0 \leq x < 1.1$ were observed at RT. Bragg's law was used to index the highest peak in the patterns showing a reflection of (311) in each, through which the crystallite size was determined. The crystallite size of the samples increases with increasing zinc concentration but is smaller than the originally prepared $CoFe_2O_4$ NPs. It increases from 57.88 to 128.92 nm. This variation in size also helps us to observe the grain growth of Zn during the synthesis process. The crystallinity percentage decreases as shown in Table 4.3 which indicates that crystallite size decreases with the substitution of Zn in the sample which is correlated with its magnetic parameters in the next section.

Table 4.3 Crystallite size and % crystallinity of synthesized $CoFe_2O_4$ NPs as a function of Zinc content.

Sample	D (nm)	% crystallinity
$Co_{1.0}Zn_{0.0}Fe_2O_4$	128.92	84.03
$Co_{0.8}Zn_{0.2}Fe_2O_4$	57.88	80.87
$Co_{0.6}Zn_{0.4}Fe_2O_4$	58.25	81
$Co_{0.4}Zn_{0.6}Fe_2O_4$	73.38	76.27
$Co_{0.2}Zn_{0.8}Fe_2O_4$	68.82	74.13

4.2 Vibrating Sample Magnetometer

VSM is used at RT to measure magnetization curves of $CoFe_2O_4$ NPs.

4.2.1 Magnetic Properties of Cobalt Ferrite Nanoparticles

(a) pH Variation

A series of $CoFe_2O_4$ NPs have been prepared by fixing the reaction temperature at 90 ^oC and varying pH from 10 to 13. M_s of samples ranges from 13.69 - 33.13 emu/g as shown in Table 4.4 (a). This change in saturation magnetization because of the change in occupancy of Co^{2+} ions at tetrahedral site may be due to change in its crystallite size or crystallinity of the sample. The hysteresis loop was traced and it was observed that there is an increasing trend of coercivity of samples ranging from 16.02 to 1247.32 Oe and then decreases. Similarly remanence ranges from 0.14 to 11.63emu/g

indicating a increasing trend and then decreases. All these observed values and the corresponding hysteresis loops are shown in Table 4.4 and Figure 4.4 respectively.

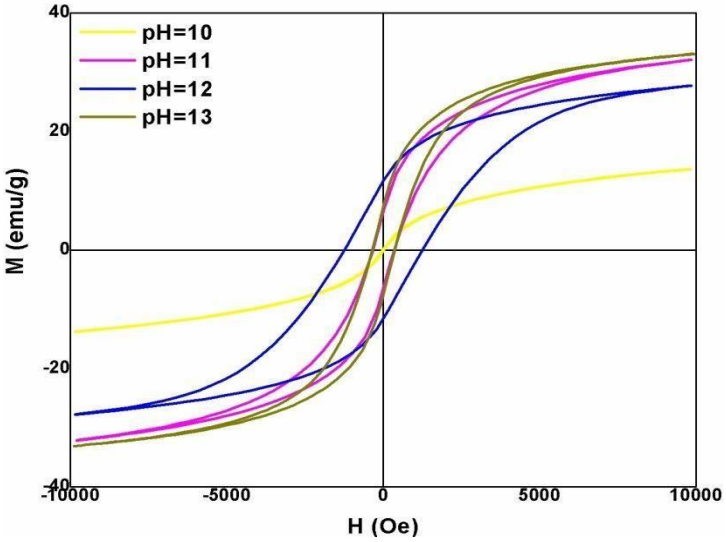

Figure 4.4 Magnetization curves of $CoFe_2O_4$ NPs prepared at 90 ^oC and pH at 10, 11, 12 and 13.

(b) Reaction Temperature Variation

A series of $CoFe_2O_4$ nanoparticles have been prepared by fixing pH at 11 and varying the reaction temperature i.e. 25 °C, 80 °C, 90 °C and 100 °C.

Table 4.4 Magnetic parameters of $CoFe_2O_4$ NPs prepared at (a) variation in pH and (b) variation in temperature.

Set	Reaction temp. (^oC)	pH	M_s (emu/g)	H_c (Oe)	M_r (emu/g)
(a)	90	10	13.69	16.02	0.14
	90	11	32.13	344.80	6.34
	90	12	27.63	1247.32	11.63
	90	13	33.13	358.26	7.45
(b)	25	11	24.58	351.75	4.77
	80	11	10.54	88.49	0.73
	90	11	32.13	344.80	6.34
	100	11	40.31	431.14	8.99

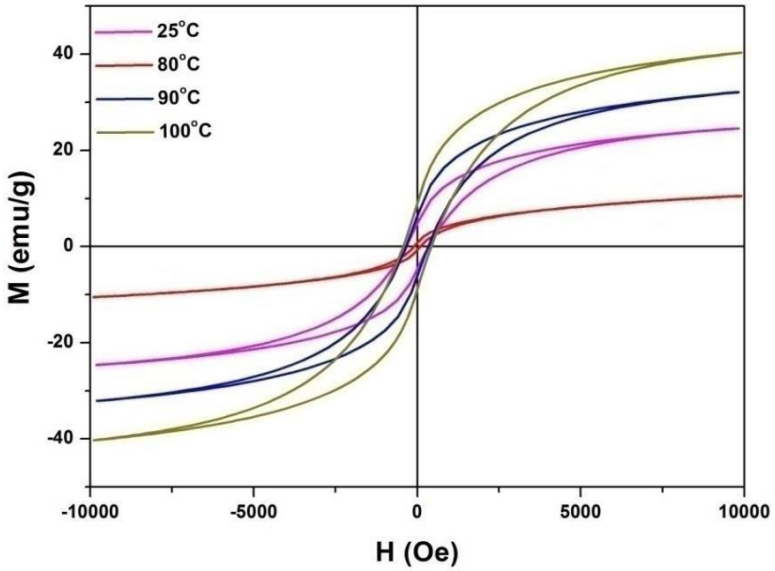

Figure 4.5 Magnetization curves of $CoFe_2O_4$ NPs prepared with pH at 11 and reaction temperature i.e. 25 °C, 80 °C, 90 °C and 100°C.

The hysteresis loops of each of these samples are shown in Figure 4.5. The pH was fixed at 11 because we got the best results from this set as discussed in Section 4.1.1 (a). M_s of samples ranges from 10.54 to 40.31 emu/g and is maximum at 100°C. The value of coercivity ranges from 88.49 to 431.14 Oe while H_r ranges from 0.73 to 8.99 emu/g. These properties show no particular trend with increasing reaction temperature. All these mentioned values are shown in Table 4.4 (b).

(c) Effect of Annealing Temperature

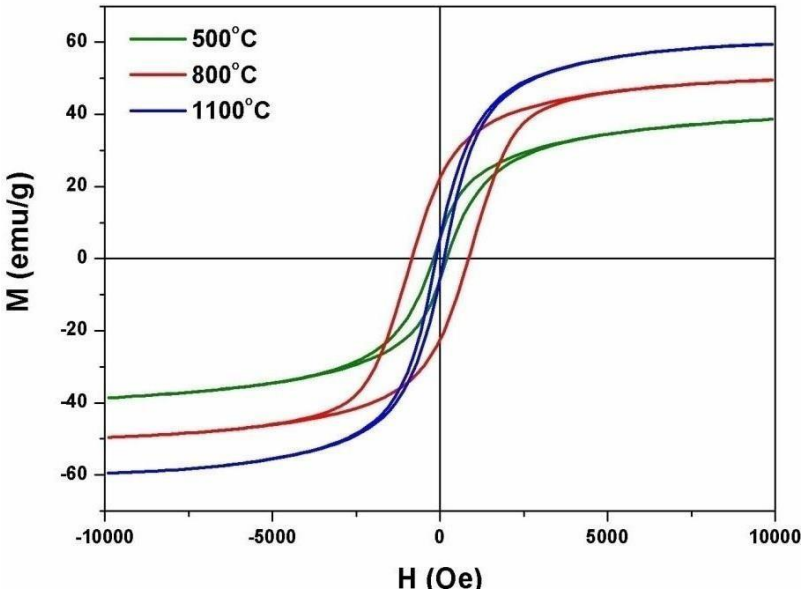

Figure 4.6 Magnetization curves of $CoFe_2O_4$ NPs annealed at 500 °C, 800 °C and 1100 °C.

The prepared sample of cobalt ferrite NPs with pH at 11 and reaction temperature at 90 ^{o}C undergo annealing at temperatures 500 ^{o}C, 800 ^{o}C and 1100 ^{o}C for 12 hrs. The respective hysteresis loops are shown in Figure 4.6 and their varying magnetic properties with annealing temperatures are listed in Table 4.5. Clearly with increase in annealing temperature, M_s also increases. This result attributes to the cobalt ferrite particles of nanosize having large surface area and therefore higher surface energy. The maximum value of saturation magnetization observed was 59.47emu/g at a annealing temperature of 1100 ^{o}C.

Table 4.5 Magnetic parameters of $CoFe_2O_4$ NPs annealed at different temperatures i.e. 500 ^{o}C, 800 ^{o}C and 1100 ^{o}C.

Set	Annealing Temp. (^{o}C)	M_s (emu/g)	H_c (Oe)	M_r (emu/g)
(c)	500	38.63	196.77	5.60
	800	49.58	854.16	22.45
	1100	59.47	112.82	5.70

From Table 4.5, we infer that there is a high dependence of magnetic parameters on annealing temperature. The value of coercivity ranges from 112.82 to 854.16 Oe, having a different variation from the other listed magnetic properties. On the other hand, value of M_r ranges from 5.60 upto 22.45 emu/g.

4.2.2 Zinc substitution in Cobalt Ferrite Nanoparticles

Typical hysteresis loops for the $CoFe_2O_4$ nanoparticle samples substituted with varying zinc content are shown in Figure 4.7. It is observed that there is no hysteresis in the sample irrespective of the amount of Zn content added, indicating their superparamagnetic behaviour. From Table 4.6, it is observed that saturation magnetization increases from 32.13- 38.98 emu/g for the samples $Co_{1.0}Zn_{0.0}Fe_2O_4$, $Co_{0.8}Zn_{0.2}Fe_2O_4$and $Co_{0.6}Zn_{0.4}Fe_2O_4$. This is because the Zn^{2+} ions replace the ones occupying the tetrahedral A-sites, resulting in a reduced magnetic moment of the sub-lattice. This further prompts an expansion in the total magnetic moment.

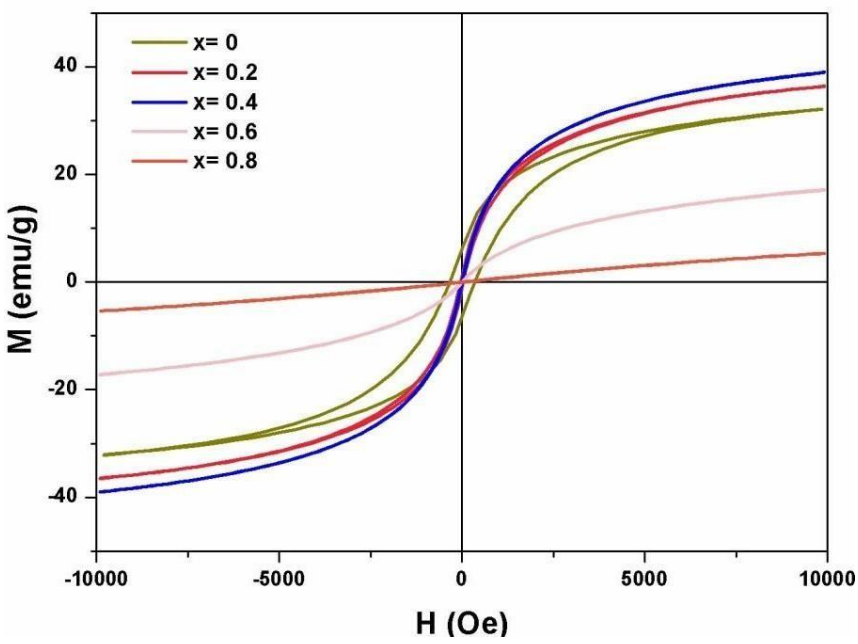

Figure 4.7 Hysteresis loops of $Co_{1-x}Zn_xFe_2O_4$ samples with $0 \leq x < 1$.

Subsequently we observe a decrease in M_s from 17.17- 5.36 emu/g in samples $Co_{0.4}Zn_{0.6}Fe_2O_4$ and $Co_{0.2}Zn_{0.8}Fe_2O_4$. This can be explained due to the fact that when Zn^{2+} ion concentration is increased above 0.4, the exchange interaction amongst tetrahedral and octahedral sites is reduced. This results the B-B interaction to gain more strength while A-B interaction to weaken, which ultimately leads in decreasing M_s.In addition, increase of zinc content also increases its diamagnetic contribution leading to decrease in their saturation magnetization. Along these lines it can be seen that the level of Zn substitution plays a noteworthy part in saturation magnetization of zinc substituted cobalt ferrite nanoparticles.

Table 4.6 Saturation magnetization of $Co_{1-x}Zn_xFe_2O_4$ NPs with varying Zinc content as x = 0, 0.2, 0.4, 0.6 and 0.8.

Sample	M_s(emu/g)
$Co_{1.0}Zn_{0.0}Fe_2O_4$	32.13
$Co_{0.8}Zn_{0.2}Fe_2O_4$	36.40
$Co_{0.6}Zn_{0.4}Fe_2O_4$	38.98
$Co_{0.4}Zn_{0.6}Fe_2O_4$	17.17
$Co_{0.2}Zn_{0.8}Fe_2O_4$	5.36

CHAPTER 5

CONCLUSION AND SCOPE FOR FUTUTRE WORK

Coprecipitation method was used for the synthesis of cobalt ferrite nanoparticles under various reaction conditions. Its structural and magnetic properties were studied by their characterization using XRD and VSM techniques. The variation in pH, reaction temperature and zinc substitution during the process of synthesis was found to be very crucial for the progression of different sizes of nanoparticles. The different reaction temperature, pH, annealing temperature and zinc substitution affects the crystallite size as well as the magnetic properties (Ms, Mr, Hc) of the synthesized nanoparticles. All the observed values significantly differ from their bulk counterparts due to quantum size effect. $CoFe_2O_4$ nanoparticles show hysteresis loops indicating that they are ferrimagnetic irrespective of the synthesis conditions. Zn substitution in $CoFe_2O_4$ nanoparticles transform them to superparamagnetic indicating that the substitution of Zn inhibits the grain growth resulting into the single domain nanoparticles.

In another interesting result, as-synthesized $CoFe_2O_4$ nanoparticles, when annealed, show temperature (of annealing) dependent magnetic properties. As the annealing temperature increases, the saturation magnetization of nanoparticles increases, while an unusual trend is observed in corresponding coercivity and remanence, which peaks at an annealing temperature of 800 ^{0}C.

Scope for future work:

- A high temperature VSM study to determine the correlation between Curie temperature and processing parameters.
- A slow scan full spectrum XRD study and its analysis to determine occupancies at tetrahedral and octahedral sites.
- Establish correlation between magnetic properties and corresponding changes in lattice structures.
- Establish the role of Zn in substituted $CoFe_2O_4$ nanoparticles towards its microstructural properties and magnetic properties.

REFERENCES

[1] J.Pérez-Arantegui, J. Molera, A. Larrea, T. Pradell, M. Vendrell -Saz, I. Borgia, B. G. Brunetti, F. Cariati, P. Fermo, M. Mellini, A. Sgamellotti, and C. Viti, *"Journal of American Chemical Society".* 84 (2004) 442-446

[2] M. Das, K. H. Shim, S. S. A. An, *"Toxicology and Environmental Health Sciences",* 3.4 (2011) 193-205.

[3] P. J. Thomas, O. L. Armstrong, S. N. Baxter, "*Metal Nanoparticles and Clusters*", Springer, Cham (2018) 31-54

[4] G. Bredig, *"Journal of Applied Chemistry"*, 41 (1898) 951-953

[5] R. Zsigmondy, *"Journal of Physical Chemistry"*,56 (1906) 77-82

[6] F. Gazeau, J. C. Bacri, F. Gendron, R. Perzynski, Y. L. Raikher, V. I.Stepanov,E. Dubois, *"Magnetism and Magnetic Materials"*, 186 (1998) 175

[7] U. Vautrin, Christine, *"Nanosciences and Nanotechnology",* Springer, Cham, (2016) 113-174

[8] B. N. Piancciola, E. L. Jr., H. E. Troiani, L. C. C. M. Nagamine, R. Cohen, R. D. Zysler, *"Journal of Magnetism and Magnetic Materials"*, 377 (2015) 44

[9] M. Mohl, K. Krisztián, *" Springer Handbook of Nanomaterials"*, Springer, Berlin, Heidelberg (2013) 389-408

[10] A. H. Lu, E. L. Salabas, and F. Schüth, *"Journal of American Chemical Society",* 46 (2007) 1222-1244

[11] N. K. Devaraj, B. H. Ong, M. Matsumoto, *"Synthesis and Reactivity in Inorganic, Metal-Organic and Nano-Metal Chemistry",* 38 (2008) 208-211

[12] M. Mozaffari, J. Amighian, E. Darsheshdar, *"Journal of Magnetism and Magnetic Materials"*, 350 (2014) 19-22

[13] M. Meshram, N. K. Agarwal, B. Sinha, P. S .Mishra, *"Journal of Magnetism and Magnetic Materials"*, 271 (2004) 207-214

[14] K. Maaz, A. Mumtaz, S. K. Hasanain, A. Ceylan, *"Journal of Magnetism and Magnetic Materials"*, 308 (2007) 289-295

[15] C. Fei, Y. Zhang, Z. Yang, Y. Liu, R. Xiong, J. Shi, X. Ruan, *" Journal of Magnetism and Magnetic Materials"*,323 (2011) 1811-1816

[16] F. S. Li, L. Wang, Q. G. Zhou, X. Z. Zhou, H. P. Kunkel,G.Williams,*"Journal of Magnetism and Magnetic Materials"*, 268 (2004) 33-39

[17] C. Liu, B. Zou, A. J. Rondinone, Z. J. Zhang, *"Journal of American Chemical Society"*, 122 (2000) 6263-6267

[18] A. Franco, V. Zapf, *"Magnetism and Magnetic Materials"*,320 (2008) 709-713

[19] I. Sharifi, H. Shokrollahi, M. M. Doroodmand, R. Safi, *"Journal of Magnetism and Magnetic Materials"*,324 (2012) 1854-1861

[20] L. D. Tung, V. Kolesnichenko, D. Caruntu, N.H. Chou, C.J. O'Connor, *" Journal of Applied Physics*", (2003) 7486-7488.

[21] I. Sharifi, H. Shokrollahi, M. M. Doroodmand, R. Safi, *"Magnetism and Magnetic Materials"*,324 (2012) 1854-1861

[22] A. Franco, Jr. and F. C. e Silva, "*Journal of Applied Physics*", 113 (2013) 17B5131-17B5133

[23] D. Zhao, X. Wu, H. Guan, E. Han, "*The Journal of Supercritical Fluids",* 42 (2007) 226-233

[24] M.G. Naseri, E.B. Saion, H.A. Ahangar, A.H. Shaari, M. Hashim, " *Journal of Nanomaterials",*2010 (2010) 75

[25] C. Vazquez, M.A.L. Quintela, M.C.B. Nunez, J. Rivaz , "*Journal of Nanoparticle Research",* 13 (2011) 1663-1676

[26] K. Gandha, K. Elkins, N.Poudyal, J.P. Liu, " *Journal of Applied Physics",* 117 (2015) 17A7361-17A7464

[27] B. G. Toksha, S. E. Shirsath, S. M. Patange, K. M. Jadhav, *"Solid State Communications"*,147 (2008) 479-483

[28] S. Singhal, T. Namgyal, S. Bansal, K. Chandra, "*Journal of Electromagnetic Analysis and Applications",* 2 (2010) 376-381

[29] M. Sajjia, M. Oubaha, M. Hasanuzzaman, A.G. Olabi,"*Ceramics International",* 40 (2014) 1147-1154

[30] A.V. Raut, R.S. Barkule, D.R. Shengule, K.M. Jadhav, "*Journal of Magnetism and Magnetic Materials",*358 (2014) 87-92

[31] T. Prabhakaran, J. Hemalatha, "*Ceramics International",* 42 (2016) 14113-14120

[32] A. H. Ashour, A. I. El –Batal, M. I. A. Abdel Maksoud, G .S. El -Sayyad, S. Labib, E. Abdeltwab, M. M. El- Okr, "*Particuology*"(2018)

[33] V. P. Senthil, J. Gajendiran, S. G. Raj, T. Shanmugavel, G.R. Kumar, C.P. Reddy, "*Chemical Physics Letter",* 695 (2018) 19-23

[34] P. C. Moaris, V. K. Garg, A. C. Oliveria, L. P. Silva, R. B. Azevedo, A. M. L. Silva, E.C.D. Lima, "*Journal of Magnetism and Magnetic Materials",* 225 (2001) 37- 40

[35] C. N. Chinnasamy, B. Jeyadevan, O.P. Perez, K. Shinoda, K. Tohji, A. Kasuya, "*IEEE Transactions on Magnetics"*, 38 (2002) 2640-2642

[36] Y. Kim, D. Kim, C. S. Lee, *"Physica B: Condensed Matter"*,337 (2003) 42-51

[37] Y. Qu, H. Yang, N. Yang, Y. Fan, H. Zhu, G. Zou, "*Materials Letters",* 60 (2006) 3548-3552

[38] I.H. Gul, A.Z. Abbasi, F. Amin, M.A. Rehman, A. Maqsood, " *Journal of Magnetism and Magnetic Materials",* 311 (2007) 494-499

[39] Z. Zi, Y. Sun, X. Zhu, Z. Yang, J. Dai, W. Song, *"Journal of Magnetism and Magnetic Materials"*, 321 (2009) 1251-1255

[40] Y. Zhang, Z. Yang, D. Yin, Y. Liu, C. Fei, R. Xiong, J. Shi, G. Yan, *"Journal of Magnetism and Magnetism Materials"*,322 (2010) 3470-3475

[41] M. Mozaffari, S. Manouchehri, M.H. Yousefi, J. Amighian, "*Journal of Magnetism and Magnetic Materials",* 322 (2010) 383-388

[42] M. M. E. Okr, M. A. Salem, M. S. Salim, R. M. E. Okr, M. Ashoush, H. M. Talaat, *"Journal of Magnetism and Magnetic Materials"*, 323 (2011) 920-926

[43] F. Huixia, C. Baiyi, Z. Devi, J. T. Lin, *"Journal of Magnetism and Magnetic Materials"*, 356 (2014) 68-72

[44] T. Tatarchuk, M. Bououdina, W. Macyk, O. Shyichuk, N. Paliychuk, I. Yaremiy, B. Najar, M. Pacia, "*Nanoscale Research Letters",* 12 (2017) 141

[45] G. A. Dorofeev, A. N. Streletskii, I. V. Povstugar, A. V. Protasov,E. P. Elsukov,*"Colloid Journal"*, 74 (2012) 675-685

[46] S. Kelutia, L. Saneblidze, V. Mikelashvili, J. Markhulia, R. Tatarashvili, D. Daraselia, D. Japaridze, *"Synthesis of Nanoparticles for Biomedical Applications"*, 4 (2015) 33-36